

A Two-Stage Iterative method for Hybrid Precoding in Downlink Millimeter Wave Massive MIMO

Mahesh Mudavath^{1,*}, S. Sandhya Rani², Dubbaka Shirisha¹ and Banoth Srinu¹

¹Electronics and Communication Engineering, Siddhartha Institute of Technology & Sciences, Ghatkesar, Hyderabad-500088, India

²Electronics and Communication Engineering, Jayamukhi Institute of Technological Sciences, Narsampet, Warangal-506332, India.

Received 3 February 2024; Accepted 27 April 2025

Abstract

At millimeter wave (mmWave) frequencies, distributed massive multiple-input multiple-output (MIMO) efficiently manages data transfer across several antennas and base stations (BSs) situated at different locations by combining analog and digital precoding. This method enhances spectral efficiency despite having less complexity and cost compared fully digital systems. This paper presents a fully connected hybrid precoding design for a downlink mmWave distributed massive multi-user MIMO. The objective function for the optimization problem is the spectral efficiency of the proposed system, subject to constraints on analog radio frequency (RF) precoding and power budget. The main aim is to maximize spectral efficiency. Due to the nonconvex nature of the problem, a two-stage iterative algorithm is proposed to determine the optimal analog and digital beamforming matrices and sum rate. The first stage obtains the optimal digital matrix assuming the analog RF precoder matrix is known, followed by acquiring the optimal analog RF precoder matrix in the next step. The Lagrange multipliers and Karush–Kuhn–Tucker (KKT) conditions for each maximization problem are computed and examined to derive the solving algorithms for each stage. The problem is then simplified, and the proposed algorithms are formulated. The simulation results demonstrate that the proposed design outperforms current methods in sum rate and approaches the performance of fully digital systems with reduced complexity compared to other alternatives.

Keywords: massive MIMO, Downlink, Hybrid precoding, Multi-user, Optimization

1. Introduction

MmWave is also known as millimeter wave, is perfectly suited for massive MIMO systems. Within the realm of massive MIMO systems, mmWave technology provides numerous advantages [1]. The wide bandwidth offered by mmWave frequencies enables the transmission of large volumes of data at high speeds [2-4]. This characteristic is crucial in a massive MIMO system as it supports many antennas. Additionally, mmWave signals have shorter wavelengths, allowing for more antennas to be accommodated in a smaller space. Consequently, this enables enhanced spatial multiplexing, facilitating the simultaneous transmission of multiple data streams across different channels. MmWave signals possess strong directional properties, making them well-suited for beamforming techniques in massive MIMO systems. Since the strong directional nature of mmWave signals, interference between adjacent cells or users can be minimized, thereby improving network capacity and reliability.

As we transition to mmWave frequencies, the propagation characteristics change significantly because of higher path attenuation. These challenges necessitate advanced approaches to maintain the performance gains provided by massive MIMO systems. The use of hybrid precoding has gained attention as a promising solution to address these issues, allowing for efficient resource

allocation in mmWave systems while reducing hardware [5]. This technique combines analog and digital precoding methods, allowing for efficient resource allocation while minimizing hardware complexity by leveraging both domains. hybrid precoding can effectively manage the trade-offs between performance and cost, making it particularly suitable for mmWave distributed multi-user (MU) massive MIMO systems. In mmWave systems, the use of hybrid precoding can significantly enhance the system's ability to serve multiple users simultaneously. Analog precoding utilizes phase shifters to manipulate signals before transmission, while digital precoding optimizes signal processing at the baseband level [6]. This dual approach is crucial in maximizing spatial diversity and improving overall system performance.

In traditional massive MIMO systems, a single BS is equipped with a large number of antennas. In distributed massive MIMO, multiple BSs are deployed over a larger area, each has a less quantity of antennas. This distribution allows for better coverage and capacity. The base stations in a distributed system can coordinate their operations to manage interference and optimize performance. This coordination can be achieved through techniques like joint processing, where signals from different base stations are processed collectively. Each base station can focus on serving users in its vicinity, leading to improved signal quality and reduced latency. This is particularly beneficial in densely populated areas where user demand is high. By having base stations spread out, the system can exploit spatial diversity more effectively [7]. This helps mitigate

*E-mail address: mahichauhan@gmail.com

ISSN: 1791-2377 © 2025 School of Science, DUTH. All rights reserved.

doi:10.25103/jestr.182.18

fading and improves overall reliability. Coordinated transmission among distributed BSs can minimize inter-cell interference, leading to higher data rates and improved Quality of Service (QoS) [8]. Distributed BSs can assist in load balancing by dynamically allocating resources based on user demand and channel conditions, ensuring efficient use of network resources. The base stations need reliable backhaul connections to communicate with a central controller or network core. This connectivity is crucial for coordinating operations and managing data traffic and usually fiber optical is used.

There are difficulties with integrating hybrid precoding in distributed systems that need to be resolved. Hardware limitations and channel state information (CSI) must be taken into account when designing efficient precoding methods [9]. In order to maximize performance, the hybrid precoding matrix must also be optimized by striking a balance between analog and digital components. When assessing hybrid precoding in mmWave distributed MU large MIMO systems, performance indicators are essential. When evaluating the overall efficacy of a system, metrics such as energy efficiency, spectrum efficiency, and user fairness are crucial. Gaining a greater understanding of how these metrics interact will help with system design and optimization tactics.

Recent revisions have focused on developing robust algorithms for hybrid precoding that can adopt to varying channel conditions and user distributions. Techniques such as alternating optimization and deep learning (DL) [10] have shown promise in improving algorithm efficiency. [11] presents effective alternating minimization (AltMin) techniques for two distinct hybrid precoding configurations: fully connected and partially connected. To emulate the performance of fully digital precoding, an AltMin algorithm utilizing manifold optimization is recommended for the fully connected framework. AltMin algorithm is subsequently applied. Additionally, for partially connected, the mentioned method with the aid of semidefinite relaxation is applied. These AltMin algorithms are then adopted for practical implementation in wideband scenarios. The phased zero forcing (PZF) is a hybrid precoding method presented in [12], which aims to achieve nearly optimal performance in massive MIMO systems. PZF manages only the phase at the radio frequency domain. Since the power limitation and cost, fully digital beamforming approaches face challenges in large-scale antenna arrays, as explored in [13]. To address this, a hybrid beamforming (HBF) architecture that combines digital and analog components is proposed to achieve similar performance with fewer RF chains. The study shows that with twice the number of RF chains as data streams, the hybrid structure can achieve the same level of performance as a fully digital beamformer. Furthermore, the mentioned paper discusses design challenges for specific scenarios and suggests heuristic solutions. Lastly, the proposed algorithms are adjusted to enable practical implementation. The research paper [14] introduces HBF algorithms designed to maximize spectral efficiency in wideband scenarios in mmWave massive MIMO using a partially connected scheme. The introduced system makes tradeoff between the problem of maximizing spectral efficiency and a Weighted MMSE problem approach. The paper breaks down the equivalent WMMSE problem, suggests solutions for optimal digital precoding and combining, and puts forward algorithms for the more complex analog precoder and combiner. The HBF algorithms have been demonstrated to enhance spectral

efficiency and exhibit convergence. Furthermore, the paper also introduces modified algorithms with reduced complexity and proposes the use of finite-resolution phase shifters.[15] addresses the difficulties associated with channel estimation and beamforming within a MU massive MIMO framework, presenting a DL-based Hybrid Beamformer as a solution tailored for 5G communication systems. This innovative design emphasizes precise channel estimation through machine learning techniques and the design of a hybrid beamformer using Neural networks. It tackles the challenges posed by low signal-to-noise ratio (SNR) conditions via the Improved Proximal Policy Optimization (IPPO) algorithm.

This manuscript proposes a hybrid precoding scheme for a distributed millimeter-wave multi-user massive MIMO system from the transmitter's perspective. Our focus is on a fully structured and distributed BS setup, where the BS is partitioned into multiple small-cell BSs (SBSs), each equipped with various antennas. We employ a two-stage iterative algorithm to maximize spectral efficiency. In the first stage, we obtain the optimal digital precoder matrix under the assumption of knowing the radio frequency (RF) precoder matrix. Subsequently, we derive the optimal RF precoder matrix using the obtained optimal digital precoder matrix. In conclusion, the primary contributions of this study are outlined as follows:

- We are examining a distributed system with mmWave multi-user massive MIMO, as a distributed structure has shown better performance compared to a collocated one [15]. Our focus is on a distributed BS scheme, comprising several SBSs, serving multiple users with numerous antennas in a fully connected configuration. To our knowledge, only a few hybrid precoding efforts have been undertaken for distributed schemes.
- we form a uniform linear array (ULA) for the configuration of antennas and develop the corresponding system model within the context of mmWave wireless communication channels. Additionally, we demonstrate that a notable rise in the quantity of transmitter antennas leads to the complete elimination of inter-user interference. Consequently, in our calculations of spectral efficiency, we exclude the term associated with inter-user interference.
- We develop a two-stage iterative algorithm to address the optimization problem. The main objective is to enhance spectral efficiency while adhering to constraints imposed by the RF precoder matrix and total power limits. In the initial phase, we assume the RF precoder is predetermined, allowing us to derive the optimal digital precoder matrix through the optimization framework. In the subsequent phase, we determine the optimal RF precoder. To adopt the iterative algorithm in both phases, we establish the Lagrange multipliers for each optimization scenario and apply the Karush-Kuhn-Tucker (KKT) conditions, subsequently calculating the desired optimal matrix. Finally, we execute the iterative algorithm for each phase.
- In the simulation section, we initially compare the spectral efficiency performance of distributed massive MIMO with the collocated system. As expected, the distributed scheme demonstrates superior performance. We also evaluate the proposed algorithm across various scenarios, including different SNRs, numbers of data streams, users, and SBS antennas. Our findings indicate that the proposed algorithm exhibits better spectral

efficiency performance compared to other existing hybrid beamforming algorithms such as analog beamforming, orthogonal matching pursuit (OMP) [22-23], and PE-AltMin [11]. It is important to note that the proposed algorithm performs exceptionally well, particularly when the number of RF chains is double the number of data streams. Furthermore, we conduct tests to confirm the convergence of the proposed algorithm, which demonstrates that the algorithm converges after a few iterations. When compared to other algorithms, the proposed scheme has lower complexity, making it a suitable low-complexity algorithm.

2. System Model

Take into account the downlink distributed massive multi-user (MU) MIMO system as shown in Fig. 1. Where the BS is divided into N SBSs. Each SBS has M antennas and N_{RF} RF chains. These SBSs simultaneously serve K users, each of which has P antennas. Furthermore, it is assumed that all SBSs are connected to a central processing unit.

This paper aims to develop a hybrid precoding for the specified system model at the transmitter side, as depicted in Fig.2. The symbol \mathbf{s}_k represents a $q \times 1$ column-vector of symbols intended for the k th user, where k ranges from 1 to K . The vector $\mathbf{s} \triangleq [\mathbf{s}_1^T, \mathbf{s}_2^T, \dots, \mathbf{s}_K^T]^T$ denotes the transmitted symbols of length $N_{sym} \triangleq Kq$. In the illustration in Fig.2,

each SBS uses an $N_{RF} \times N_{sym}$ digital baseband precoding matrix, denoted by $\mathbf{F}_{BB_i} = [\mathbf{F}_{BB_{i,1}}, \mathbf{F}_{BB_{i,2}}, \dots, \mathbf{F}_{BB_{i,K}}]$, $0 \leq i \leq N$, to precode the symbols vector. The resulting streams are then upconverted to the radio frequency in the N_{RF} RF chains. These analog signals are subsequently phase-shifted using an $M \times N_{RF}$ analog RF precoder denoted by \mathbf{F}_{RF_i} before being transmitted to the users using the SBS's M antennas.

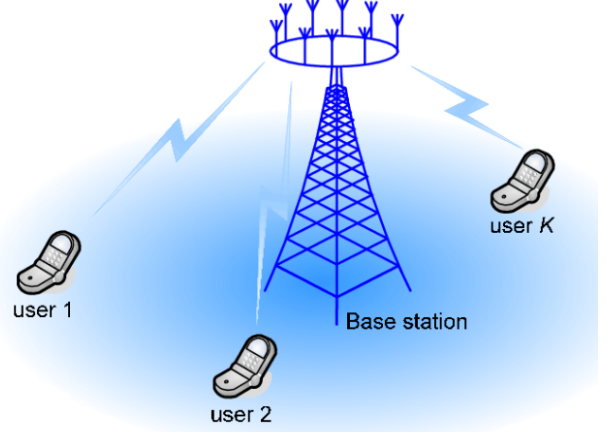


Fig. 1. The considered downlink distributed massive MU-MIMO system model

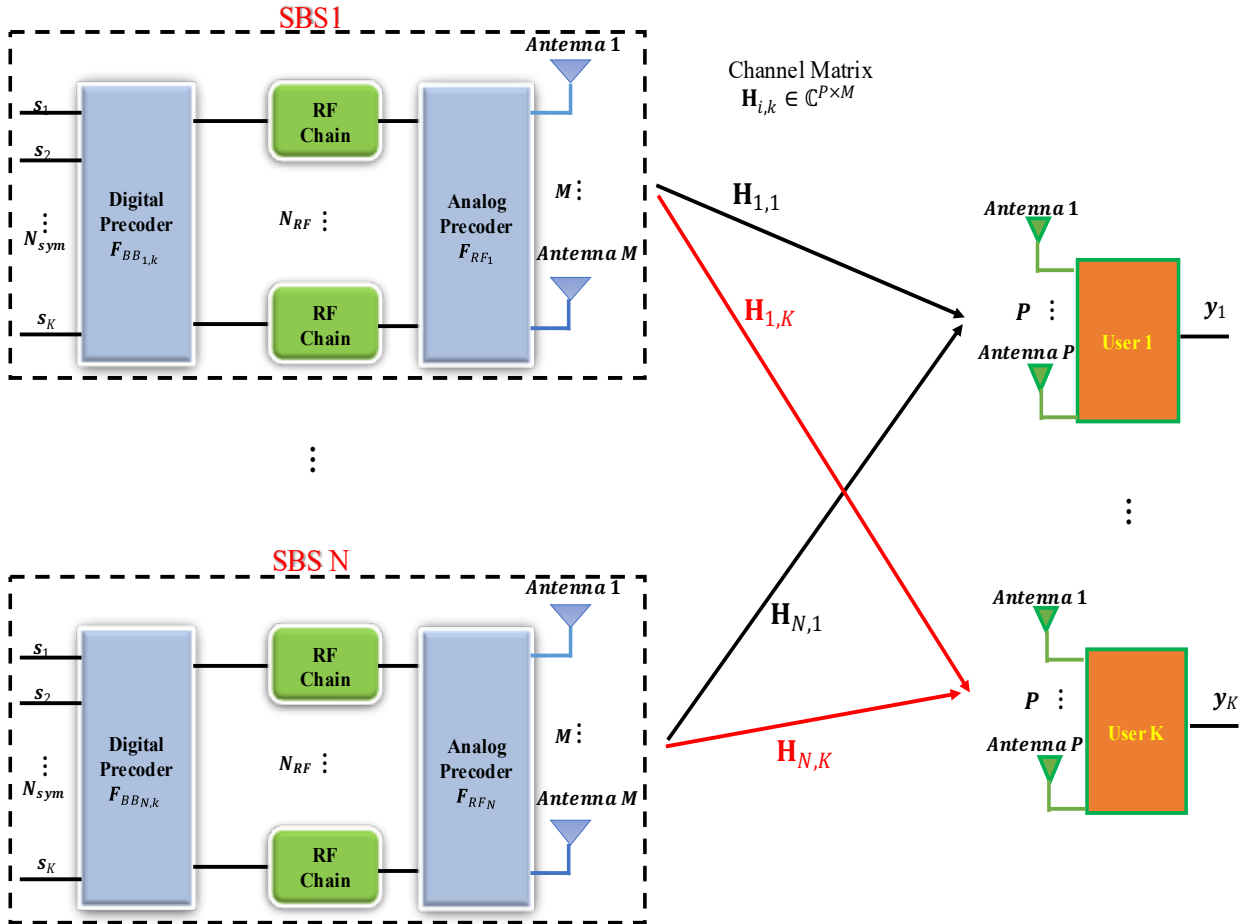


Fig. 2. The downlink distributed massive MU-MIMO system with fully connected hybrid precoding at transmitter (SBS) side

The signal transmitted in each SBS can be represented as follows:

$$\mathbf{x}_i = \mathbf{F}_{RF_i} \mathbf{F}_{BB_i} \mathbf{s} \quad (1)$$

In the above equation, it is assumed that $\mathbf{s}_1, \mathbf{s}_2, \dots, \mathbf{s}_K$ are orthogonal, and i shows the number of SBSs. Additionally, the signal received by user k can be represented as:

$$\mathbf{y}_{i,k} = \mathbf{H}_{i,k} \mathbf{F}_{RF_i} \mathbf{F}_{BB_{i,k}} \mathbf{s}_k + \sum_{l \neq k} \mathbf{H}_{i,k} \mathbf{F}_{RF_i} \mathbf{F}_{BB_{i,l}} \mathbf{s}_l + \mathbf{z}_k \quad (2)$$

$$\mathbf{y}_k = \sum_{i=1}^N (\mathbf{H}_{i,k} \mathbf{F}_{RF_i} \mathbf{F}_{BB_{i,k}} \mathbf{s}_k + \sum_{l \neq k} \mathbf{H}_{i,k} \mathbf{F}_{RF_i} \mathbf{F}_{BB_{i,l}} \mathbf{s}_l) + \mathbf{z}_k \quad (3)$$

Where $\mathbf{H}_{i,k}$ is the $P \times M$ channel matrix from the transmit antennas of each SBS to the k th user and $\mathbf{z}_k \sim \mathcal{CN}(\mathbf{0}, \sigma^2 \mathbf{I}_P)$ represents the additive white Gaussian noise.

3. Channel Model

The channel between the i -th SBS and k -th user is characterized by $\mathbf{H}_{i,k} = \sqrt{\beta_{i,k}} \dot{\mathbf{H}}_{i,k}$. The term $\sqrt{\beta_{i,k}}$ denotes the large-scale fading, while $\dot{\mathbf{H}}_{i,k}$ represents the fast fading. In this context, we are considering the mmWave channel with limited scattering and a finite number of propagation paths, denoted as L_k , where $k = \{1, 2, \dots, K\}$. This is defined [5]:

$$\dot{\mathbf{H}}_{i,k} = \sqrt{\frac{PM}{L_k}} \sum_{l=1}^{L_k} \alpha_{i,k,l} \mathbf{a}_R(\theta_{i,k,l}) \mathbf{a}_T^H(\phi_{i,k,l}) \quad (4)$$

The notation $\alpha_{i,k,l}$ denotes the path fading coefficient associated with the l -th path for the k -th user within the i -th SBS. This coefficient is characterized by a complex Gaussian distribution, exhibiting a mean of zero and a variance of one. Within the context of the i -th SBS, the angles of arrival and departure (AoA/AoD) for the l -th path corresponding to the k -th user are represented by $\theta_{i,k,l}$ and $\phi_{i,k,l}$, respectively. Additionally, the receive and transmit array response vectors at these specified azimuth angles are denoted as $\mathbf{a}_R(\theta_{i,k,l})$ and $\mathbf{a}_T(\phi_{i,k,l})$. It is assumed that all the values of $\theta_{i,k,l}$ and $\phi_{i,k,l}$ are uniformly distributed on the interval $[0, 2\pi)$, and the antennas in each user have a uniform linear array (ULA) arrangement. The formulations for $\mathbf{a}_R(\theta_{i,k,l})$ and $\mathbf{a}_T(\phi_{i,k,l})$ are as follows:

$$\mathbf{a}_R(\theta_{i,k,l}) = \frac{1}{\sqrt{P}} \left[1, e^{-\frac{j2\pi d}{\lambda} \sin(\theta_{i,k,l})}, \dots, e^{-\frac{j2\pi(P-1)d}{\lambda} \sin(\theta_{i,k,l})} \right]^T \quad (5)$$

$$\mathbf{a}_T(\phi_{i,k,l}) = \frac{1}{\sqrt{M}} \left[1, e^{-\frac{j2\pi d}{\lambda} \sin(\phi_{i,k,l})}, \dots, e^{-\frac{j2\pi(M-1)d}{\lambda} \sin(\phi_{i,k,l})} \right]^T \quad (6)$$

Where,

λ is the carrier wavelength and d denotes the spacing between two neighbor antennas. In this paper, we assume $\lambda/2$ for d .

Proposition:

In the context of multi-user MIMO in a Massive MIMO system with a large number of transmitter antennas in a ULA configuration, the different user channels exhibit orthogonality, leading to the elimination of interference. i.e. :

$$\lim_{M \rightarrow \infty} \frac{1}{M} \mathbf{h}_a(u) \mathbf{h}_b^H(v) = 0 \quad \text{for } a \neq b, u \neq v \quad (7)$$

Where, a and b shows the different users

Proof: In this section, we are examining interference between users and aiming to demonstrate the independence of users from each other. As a result, for simplicity and without losing any generality, we will omit the index i in equation (8) and focus on the channel from a specific SBS to all users. This approach can be extended to cover all SBSs.

If $\mathbf{h}_k(w)$ denotes the channel vector of w -th antenna in k -th user for mmWave channel, the channel can be demonstrated as:

$$\mathbf{h}_k(w) = \sqrt{\frac{M}{L_k}} \sum_{l=1}^{L_k} \sqrt{\beta_k} \alpha_{k,l} e^{-j(w-1) \frac{2\pi d}{\lambda} \sin(\theta_{k,l})} \mathbf{a}_T^H(\phi_{k,l}) \quad (8)$$

By introducing $F_{l_u, u} = \sqrt{\beta_a} \alpha_{a, l_u} e^{-j(u-1) \frac{2\pi d}{\lambda} \sin(\theta_{a, l_u})}$ and $F_{l_v, v} = \sqrt{\beta_b} \alpha_{b, l_v} e^{-j(v-1) \frac{2\pi d}{\lambda} \sin(\theta_{b, l_v})}$, we can express:

$$\begin{aligned} \frac{1}{M} \mathbf{h}_a(u) \mathbf{h}_b^H(v) &= \frac{1}{\sqrt{L_u}} \sum_{l_u=1}^{L_u} F_{l_u, u} \mathbf{a}_T^H(\phi_{a, l_u}) \times \\ &\frac{1}{\sqrt{L_v}} \sum_{l_v=1}^{L_v} F_{l_v, v}^* \mathbf{a}_T(\phi_{b, l_v}) = \sqrt{\frac{1}{L_u L_v}} \sum_{l_u=1}^{L_u} \sum_{l_v=1}^{L_v} (F_{l_u, u} F_{l_v, v}^* \times \\ &\frac{1}{M} \sum_{m=1}^M e^{-j(m-1) \left(\frac{2\pi d}{\lambda} (\sin(\phi_{a, l_u}) - \sin(\phi_{b, l_v})) \right)}) \end{aligned} \quad (9)$$

To prove (7), we just need to demonstrate that the mean and variance of $\lim_{M \rightarrow \infty} \frac{1}{M} \mathbf{h}_a(u) \mathbf{h}_b^H(v)$ are both equal to zero.

Before computing the first and second moments of $\lim_{M \rightarrow \infty} \frac{1}{M} \mathbf{h}_a(u) \mathbf{h}_b^H(v)$, it is important to highlight that the expression $\frac{1}{M} \mathbf{h}_a(u) \mathbf{h}_b^H(v)$ takes the form of $e^{\pm jx \sin \gamma}$ where γ is a random variable. As per [24], if γ is uniformly distributed between 0 and 2π , then:

$$\mathbb{E}_\gamma \{ e^{\pm jx \sin \gamma} \} = \frac{1}{2\pi} \int_0^{2\pi} e^{\pm jx \sin \gamma} d\gamma = J_0(x) \quad (10)$$

Where $J_0(\cdot)$ in (10) shows the zero-order Bessel function of the first kind.

We know that all AoAs and AoDs are uniformly distributed between 0 and 2π and they are independent, therefore:

$$\begin{aligned} \mathbb{E} \left\{ \frac{1}{M} \mathbf{h}_a(u) \mathbf{h}_b^H(v) \right\} &= \\ &\sqrt{\frac{1}{L_u L_v}} \sum_{l_u=1}^{L_u} \sum_{l_v=1}^{L_v} \mathbb{E} \left\{ \sqrt{\beta_a \beta_b} \alpha_{a, l_u} \alpha_{b, l_v}^* \right\} \times \\ &J_0(x_u) J_0(x_v) \frac{1}{M} \sum_{m=1}^M J_0(x_m)^2 \end{aligned} \quad (11)$$

Where

$$x_u = \frac{2\pi d}{\lambda} (u-1), x_v = \frac{2\pi d}{\lambda} (v-1), \text{ and } x_m = \frac{2\pi d}{\lambda} (m-1).$$

Since the magnitude of $J_0(z)$ decays proportional to $\frac{1}{\sqrt{z}}$, therefore:

$$\lim_{M \rightarrow \infty} \frac{1}{M} \sum_{m=1}^M J_0(x_m)^2 = 0 \quad (12)$$

In result, it can be obtained:

$$\mathbb{E}_\gamma \left\{ \lim_{M \rightarrow \infty} \frac{1}{M} \mathbf{h}_a(u) \mathbf{h}_b^H(v) \right\} = 0 \quad (13)$$

We know that the variance of variable X is $\mathbb{E}\{(X - \mathbb{E}(X))^2\}$, therefore according to (7):

$$\text{Var}\left\{\frac{1}{M}\mathbf{h}_a(u)\mathbf{h}_b^H(v)\right\} = \mathbb{E}\left\{\frac{1}{M^2}|\mathbf{h}_a(u)\mathbf{h}_b^H(v)|^2\right\} \text{ for } M \rightarrow \infty \quad (14)$$

In additions,

$$\begin{aligned} \mathbb{E}\left\{\frac{1}{M^2}|\mathbf{h}_a(u)\mathbf{h}_b^H(v)|^2\right\} = & \sqrt{\frac{1}{L_u L_v} \sum_{l_u=1}^{L_u} \sum_{l_v=1}^{L_v} \mathbb{E}\left\{|\sqrt{\beta_a \beta_b^*} \alpha_{a,l_u} \alpha_{b,l_v}^*|^2\right\}} \times \\ & \frac{1}{M^2} \sum_{m=1}^M \sum_{m'=1}^M J_0(x_{m,m'})^2 + C \end{aligned} \quad (15)$$

Where $x_{m,m'} = \frac{2\pi d}{\lambda}(m - m')$ and $C \rightarrow 0$ if $M \rightarrow \infty$. So, by substituting (15) into (14):

$$\text{Var}\left\{\frac{1}{M}\mathbf{h}_a(u)\mathbf{h}_b^H(v)\right\} = O\left(\frac{1}{M}\right) \quad (16)$$

Where $O(x)$ shows that the value is proportional to x . Therefore:

$$\text{Var}\left\{\lim_{M \rightarrow \infty} \frac{1}{M}\mathbf{h}_a(u)\mathbf{h}_b^H(v)\right\} = 0 \quad (17)$$

4. Spectral Efficiency

This section assesses the spectral efficiency of the proposed framework. As demonstrated in the previous part, the interference among users is proven to be zero. Therefore, the total spectral efficiency of the user k in the distributed system proposed is given by:

$$R_k = \log_2 \left| \mathbf{I}_P + \frac{\sum_{i=1}^N \mathbf{H}_{i,k} \mathbf{F}_{RF_i} \mathbf{F}_{BB_i} \mathbf{F}_{BB_i}^H \mathbf{F}_{RF_i}^H \mathbf{H}_{i,k}^H}{\sigma^2} \right| \quad (18)$$

The total spectral efficiency for all users from all SBSs in the suggested system, denoted as R_{total} , is calculated by adding up the spectral efficiencies of individual users from all SBSs in the system.

$$R_{total} = \sum_{k=1}^K \log_2 \left| \mathbf{I}_P + \frac{\sum_{i=1}^N \mathbf{H}_{i,k} \mathbf{F}_{RF_i} \mathbf{F}_{BB_i} \mathbf{F}_{BB_i}^H \mathbf{F}_{RF_i}^H \mathbf{H}_{i,k}^H}{\sigma^2} \right| \quad (19)$$

The noise variance, denoted as σ^2 , is assumed to be constant in all paths, and the entity matrix is represented by \mathbf{I}_P .

5. Spectral Efficiency Optimization Problem Definition

This study seeks to enhance the total spectral efficiency while adhering to analog RF precoding and total power constraints. Our goal is to derive the best hybrid precoding (analog RF and digital) matrices at SBSs by solving the specified optimization problem:

$$\text{maximize}_{\mathbf{F}_{BB_i}, \mathbf{F}_{RF_i}} R_{total} \quad (20a)$$

$$\text{s.t. } \text{Tr}(\mathbf{F}_{RF_i} \mathbf{F}_{BB_i} \mathbf{F}_{BB_i}^H \mathbf{F}_{RF_i}^H) \leq P_T \quad (20b)$$

$$\mathbf{F}_{RF_i} \mathbf{F}_{RF_i}^H = \mathbf{I}_M \quad (20c)$$

Where, P_T is the total power budget and \mathbf{I}_M and \mathbf{I}_P are entity matrices. The system transmit power limitations are represented by the first constraint, while the second constraint is satisfied through the precoding sections.

6. Solving the Problem

The optimization problem in the previous section (20) deals with hybrid precoders at the transmitter. However, addressing this design problem for analog/digital matrices is extremely challenging [4]. Furthermore, the nonconvex constraint (20b) complicates the problem by making it non-convex. As a result, we propose a new two-stage approach to tackle this issue. First, we consider the analog RF precoding matrix to be identified and concentrate on finding the optimal digital precoding matrix. Subsequently, we use the optimal digital precoding matrix to obtain the optimal RF precoding matrix. This procedure is illustrated in Figure 3.

We assume that the analog RF precoder, \mathbf{F}_{RF_i} , is known and then compute the digital precoder, \mathbf{F}_{BB_i} . By considering this assumption, we can say that $\mathbf{H}_{i,k}^e = \mathbf{H}_{i,k} \mathbf{F}_{RF_i}$ and also the problem (20) is changed as:

$$\text{maximize}_{\mathbf{F}_{BB_i}} \sum_{k=1}^K \log_2 \left| \mathbf{I}_P + \frac{\sum_{i=1}^N \mathbf{H}_{i,k}^e \mathbf{F}_{BB_i} \mathbf{F}_{BB_i}^H (\mathbf{H}_{i,k}^e)^H}{\sigma^2} \right| \quad (21a)$$

$$\text{subject to: } \text{Tr}(\mathbf{W}_i \mathbf{F}_{BB_i} \mathbf{F}_{BB_i}^H) \leq P_T \quad (21b)$$

In above equations, we define $\mathbf{W}_i = \mathbf{F}_{RF_i}^H \mathbf{F}_{RF_i}$ to simplify the problem (20).

For solving the above problem, we utilize the Lagrange multiplier method [26].

$$\begin{aligned} \mathcal{L}(\mathbf{F}_{BB_i}, \lambda) = & \sum_{k=1}^K \log_2 \left| \mathbf{I}_P + \frac{\sum_{i=1}^N \mathbf{H}_{i,k}^e \mathbf{F}_{BB_i} \mathbf{F}_{BB_i}^H (\mathbf{H}_{i,k}^e)^H}{\sigma^2} \right| + \\ & \lambda (\text{Tr}(\mathbf{W}_i \mathbf{F}_{BB_i} \mathbf{F}_{BB_i}^H) - P_T) \end{aligned} \quad (22)$$

According KKT conditions, we have:

$$\frac{\partial \mathcal{L}(\mathbf{F}_{BB_i}, \lambda)}{\partial \mathbf{F}_{BB_i}} = 0 \quad (23)$$

$$\frac{\partial \mathcal{L}(\mathbf{F}_{BB_i}, \lambda)}{\partial \lambda} = 0 \quad (24)$$

Therefore, the (23) can be calculated as:

$$\begin{aligned} \frac{\partial \mathcal{L}(\mathbf{F}_{BB_i}, \lambda)}{\partial \mathbf{F}_{BB_i}} = & \frac{\partial \left(\sum_{k=1}^K \log_2 \left| \mathbf{I}_P + \frac{\sum_{i=1}^N \mathbf{H}_{i,k}^e \mathbf{F}_{BB_i} \mathbf{F}_{BB_i}^H (\mathbf{H}_{i,k}^e)^H}{\sigma^2} \right| \right)}{\partial \mathbf{F}_{BB_i}} + \\ & \frac{\partial \lambda (\text{Tr}(\mathbf{W}_i \mathbf{F}_{BB_i} \mathbf{F}_{BB_i}^H) - P_T)}{\partial \mathbf{F}_{BB_i}} = 0 \end{aligned} \quad (25)$$

Therefore, we can compute (I) in (25) as:

$$\begin{aligned} \text{I} = & \sum_{k=1}^K \frac{\partial}{\partial \mathbf{F}_{BB_i}} \log_2 \left| \mathbf{I}_P + \frac{\sum_{i=1}^N \mathbf{H}_{i,k}^e \mathbf{F}_{BB_i} \mathbf{F}_{BB_i}^H (\mathbf{H}_{i,k}^e)^H}{\sigma^2} \right| = \\ & \sum_{k=1}^K \frac{\partial}{\partial \mathbf{F}_{BB_i}} \log_2 \left(\frac{1}{\sigma^2} \right) + \frac{\partial}{\partial \mathbf{F}_{BB_i}} \log_2 \left| \sigma^2 \mathbf{I}_P + \right. \end{aligned}$$

$$\sum_{i=1}^N \mathbf{H}_{i,k}^e \mathbf{F}_{BB_i} \mathbf{F}_{BB_i}^H (\mathbf{H}_{i,k}^e)^H \Big| = \sum_{k=1}^K \frac{\partial}{\partial \mathbf{F}_{BB_i}} \log_2 \left| \sigma^2 \mathbf{I}_P + \sum_{i=1}^N \mathbf{H}_{i,k}^e \mathbf{F}_{BB_i} \mathbf{F}_{BB_i}^H (\mathbf{H}_{i,k}^e)^H \right| \quad (26)$$

By knowing $\text{Log}_2(x) = \frac{\ln(x)}{\ln 2}$, the (26) is changed as:

$$\frac{\partial}{\partial \mathbf{F}_{BB_i}} \sum_{k=1}^K \log_2 \left| \sigma^2 \mathbf{I}_P + \sum_{i=1}^N \mathbf{H}_{i,k}^e \mathbf{F}_{BB_i} \mathbf{F}_{BB_i}^H (\mathbf{H}_{i,k}^e)^H \right| = \frac{1}{\ln 2} \sum_{k=1}^K \frac{\partial}{\partial \mathbf{F}_{BB_i}} \left(\ln \left| \sigma^2 \mathbf{I}_P + \sum_{i=1}^N \mathbf{H}_{i,k}^e \mathbf{F}_{BB_i} \mathbf{F}_{BB_i}^H (\mathbf{H}_{i,k}^e)^H \right| \right) \quad (27)$$

We know that $(\ln(f(x)))' = \frac{f'(x)}{f(x)}$:

$$\begin{aligned} \frac{\partial}{\partial \mathbf{F}_{BB_i}} \left(\ln \left| \sigma^2 \mathbf{I}_P + \sum_{i=1}^N \mathbf{H}_{i,k}^e \mathbf{F}_{BB_i} \mathbf{F}_{BB_i}^H (\mathbf{H}_{i,k}^e)^H \right| \right) &= \frac{\frac{\partial}{\partial \mathbf{F}_{BB_i}} \left| \sigma^2 \mathbf{I}_P + \sum_{i=1}^N \mathbf{H}_{i,k}^e \mathbf{F}_{BB_i} \mathbf{F}_{BB_i}^H (\mathbf{H}_{i,k}^e)^H \right|}{\left| \sigma^2 \mathbf{I}_P + \sum_{i=1}^N \mathbf{H}_{i,k}^e \mathbf{F}_{BB_i} \mathbf{F}_{BB_i}^H (\mathbf{H}_{i,k}^e)^H \right|} \\ &= \frac{\left| \sigma^2 \mathbf{I}_P + \sum_{i=1}^N \mathbf{H}_{i,k}^e \mathbf{F}_{BB_i} \mathbf{F}_{BB_i}^H (\mathbf{H}_{i,k}^e)^H \right|^{-1} \sum_{i=1}^N \left(\mathbf{H}_{i,k}^e \right)^H \mathbf{H}_{i,k}^e \mathbf{F}_{BB_i}}{\left| \sigma^2 \mathbf{I}_P + \sum_{i=1}^N \mathbf{H}_{i,k}^e \mathbf{F}_{BB_i} \mathbf{F}_{BB_i}^H (\mathbf{H}_{i,k}^e)^H \right|} = 2 \sum_{i=1}^N \left(\mathbf{H}_{i,k}^e \right)^H \mathbf{H}_{i,k}^e \mathbf{F}_{BB_i} \end{aligned} \quad (28)$$

Therefore:

$$\begin{aligned} \frac{1}{\ln 2} \sum_{k=1}^K \frac{\partial}{\partial \mathbf{F}_{BB_i}} \left(\ln \left| \sigma^2 \mathbf{I}_P + \sum_{i=1}^N \mathbf{H}_{i,k}^e \mathbf{F}_{BB_i} \mathbf{F}_{BB_i}^H (\mathbf{H}_{i,k}^e)^H \right| \right) &= \frac{2}{\ln 2} \sum_{k=1}^K \sum_{i=1}^N \left(\mathbf{H}_{i,k}^e \right)^H \mathbf{H}_{i,k}^e \mathbf{F}_{BB_i} \end{aligned} \quad (29)$$

According to

$$\frac{\partial}{\partial \mathbf{X}} \text{Tr}(\mathbf{B}\mathbf{X}\mathbf{X}^T) = (\mathbf{B} + \mathbf{B}^T)\mathbf{X} [27],$$

the second part in (25), II, is calculated as:

$$\text{II} = \frac{\partial \lambda (\text{Tr}(\mathbf{W}_i \mathbf{F}_{BB_i} \mathbf{F}_{BB_i}^H) - P_T)}{\partial \mathbf{F}_{BB_i}} = \lambda (\mathbf{W}_i + \mathbf{W}_i^H) \mathbf{F}_{BB_i} \quad (30)$$

So, according to KKT conditions and (29) and (30):

$$\begin{aligned} \frac{\partial \mathcal{L}(\mathbf{F}_{BB_i}, \lambda)}{\partial \mathbf{F}_{BB_i}} &= 0 \Rightarrow \\ \frac{\partial \mathcal{L}(\mathbf{F}_{BB_i}, \lambda)}{\partial \mathbf{F}_{BB_i}} - \frac{2}{\ln 2} \sum_{k=1}^K \sum_{i=1}^N \left(\mathbf{H}_{i,k}^e \right)^H \mathbf{H}_{i,k}^e \mathbf{F}_{BB_i} + \lambda (\mathbf{W}_i + \mathbf{W}_i^H) \mathbf{F}_{BB_i} &= 0 \end{aligned} \quad (31)$$

According to (30), we can conclude that :

$$\mathbf{F}_{BB_i}^* = \frac{-2}{\lambda \ln 2} (\mathbf{W}_i + \mathbf{W}_i^H)^{-1} \left(\sum_{k=1}^K \sum_{i=1}^N \left(\mathbf{H}_{i,k}^e \right)^H \mathbf{H}_{i,k}^e \mathbf{F}_{BB_i} \right) \quad (32)$$

And also, based on KKT conditions:

$$\begin{aligned} \frac{\partial \mathcal{L}(\mathbf{F}_{BB_i}, \lambda)}{\partial \lambda} &= 0 \Rightarrow \\ \frac{\partial \mathcal{L}(\mathbf{F}_{BB_i}, \lambda)}{\partial \lambda} - \text{Tr}(\mathbf{W}_i \mathbf{F}_{BB_i} \mathbf{F}_{BB_i}^H) - P_T &= 0 \Rightarrow \\ \text{Tr}(\mathbf{W}_i \mathbf{F}_{BB_i} \mathbf{F}_{BB_i}^H) &= P_T \end{aligned} \quad (33)$$

Now, we should investigate the conditions and choose the suitable case for the parameter:

$$\begin{aligned} \text{if } \lambda (\text{Tr}(\mathbf{W}_i \mathbf{F}_{BB_i} \mathbf{F}_{BB_i}^H) - P_T) &= 0 \Rightarrow \\ \left\{ \begin{array}{l} \lambda = 0 \quad \text{Tr}(\mathbf{W}_i \mathbf{F}_{BB_i} \mathbf{F}_{BB_i}^H) < P_T \quad (A) \\ \lambda > 0 \quad \text{Tr}(\mathbf{W}_i \mathbf{F}_{BB_i} \mathbf{F}_{BB_i}^H) = P_T \quad (B) \end{array} \right. \end{aligned} \quad (34)$$

In (32), the λ could not be zero, because if $\lambda = 0$, $\mathbf{F}_{BB_i}^* = \infty$. So, the condition (B) in (34), $> 0 \text{Tr}(\mathbf{W}_i \mathbf{F}_{BB_i} \mathbf{F}_{BB_i}^H) = P_T$, is satisfied.

In result, our optimization problem is changed as:

$$\left\{ \begin{array}{l} \mathbf{F}_{BB_i}^* = \frac{-2}{\lambda \ln 2} (\mathbf{W}_i + \mathbf{W}_i^H)^{-1} \left(\sum_{k=1}^K \sum_{i=1}^N \left(\mathbf{H}_{i,k}^e \right)^H \mathbf{H}_{i,k}^e \mathbf{F}_{BB_i} \right) \\ \text{Tr}(\mathbf{W}_i \mathbf{F}_{BB_i} \mathbf{F}_{BB_i}^H) = P_T \end{array} \right. \quad (35)$$

For solving the problem (35), we use the proposed iterative algorithm I as follows. Note that $\mathbf{F}_{BB_i}^*$ shows the optimal \mathbf{F}_{BB_i} .

In the first step of Algorithm I, we start by setting λ_{min} and λ_{max} , and then calculate λ as $\lambda = \frac{\lambda_{max} + \lambda_{min}}{2}$. Using this initial λ , we compute $\mathbf{F}_{BB_i}^*$ for each SBS and user. If $\text{Tr}(\mathbf{W}_i \mathbf{F}_{BB_i} \mathbf{F}_{BB_i}^H) = P_T$ holds true for $\mathbf{F}_{BB_i}^*$, we update λ_{min} to λ and keep λ_{max} as is, then calculate the new λ . If the stopping condition $|\lambda_{min} - \lambda_{max}| > \epsilon$ is met, the algorithm stops and we obtain the optimal digital precoding matrix. If not, we repeat the algorithm until the optimal \mathbf{F}_{BB_i} is achieved.

Algorithm I The pseudo-code of the proposed iterative algorithm for finding \mathbf{F}_{BB_i}

1. $\lambda_{min} = 0$
2. $\lambda_{max} = \mathcal{M}$ (a large enough number)
3. ϵ is a small number
4. while (abs($\lambda_{min} - \lambda_{max}$) > ϵ)
5. $\lambda = \frac{\lambda_{max} + \lambda_{min}}{2}$
6. for $i=1$: SBS Number
7. for $k=1$: User Number
8. compute

$$\mathbf{F}_{BB_i}^* = \frac{-2}{\lambda \ln 2} (\mathbf{W}_i + \mathbf{W}_i^H)^{-1} \left(\sum_{k=1}^K \sum_{i=1}^N \left(\mathbf{H}_{i,k}^e \right)^H \mathbf{H}_{i,k}^e \mathbf{F}_{BB_i} \right)$$

9. End for
10. End for

11. compute

$$\text{Tr}(\mathbf{W}_i \mathbf{F}_{BB_i} \mathbf{F}_{BB_i}^H)$$

12. if $\text{Tr}(\mathbf{W}_i \mathbf{F}_{BB_i} \mathbf{F}_{BB_i}^H) = P_T$ %
 P_T is the total transmitted power

13. $\lambda_{min} = \lambda$
14. $\lambda_{max} = \lambda_{max}$
15. $\lambda = \frac{\lambda_{max} + \lambda_{min}}{2}$
16. else
17. $\lambda_{min} = \lambda_{min}$
18. $\lambda_{max} = \lambda$
19. $\lambda = \frac{\lambda_{max} + \lambda_{min}}{2}$

- Endif
 - End While
-

When determining the complexity of the proposed algorithm. It should be emphasized that in the distributed case, the complexity is $\frac{1}{N}$ of the collocated case, where N represents the number of SBS. This is because the antennas

are divided among N separate SBSs, making our proposed scheme less complex than other collocated schemes. However, when comparing with other algorithms without considering the BS configurations, we can calculate the complexity for one SBS and compare it with other algorithms. In this particular scenario, the complexity is $O(M \times N_{sym} \times P \times K)$. Thus, if we set $K = 1$, the complexity becomes $O(M \times N_{sym} \times P)$, which is similar to the complexity in [13]. Similarly, if we consider a multi-user scenario with $P = 1$, the complexity becomes $O(M \times N_{sym} \times K)$, which is also similar to [13]. Assuming all parameters have the same range, i.e., N_{comp} , the complexity is $O(N_{comp}^3)$, similar to [13], in both of these scenarios. For a multi-user scenario with multiple antennas, similar to our scenario, the complexity in [16] is $O(N_{comp}^5)$, and in [28] is $O(N_{comp}^6)$, while in our proposed algorithm, the complexity is $O(N_{comp}^4)$. Thus, in all the investigated cases, the proposed iterative algorithm exhibits low complexity.

7. Simulation Results

Within this part, we will assess the performance of the proposed hybrid precoding algorithm under various conditions. We will focus on a ULA configuration with antennas spaced at half the wavelength distance. Our evaluations will be conducted for a distributed massive multi-user MIMO system operating in the mmWave wireless communication channel. All simulations are executed by MATLAB software, and the results will be based on an average of 100 channel realizations. For the mmWave channel model, we will set $L_k = 3$. The AoAs and AoDs will follow a uniform distribution within the range $[0, 2\pi]$. We will use $\epsilon = 10^{-6}$ for our proposed algorithm. In most of our simulations, we will set $N = 4$, $M = 64$, $K = 6$, $P = 16$, and $N_{RF} = N_{sym}$ or $2 * N_{sym}$. However, we will adjust certain parameters for each figure based on the conditions and provide details in the figure's description. We will assume a noise variance of $\sigma^2 = 1$ for all paths, and SNR will be calculated as $\frac{P_T}{\sigma^2}$.

A comparison of spectral efficiency at various SNRs in the distributed and collocated massive MIMO setup is presented in Fig.3. As indicated in [15], it is evident that the distributed massive MIMO exhibits superior spectral efficiency, particularly when there are high quantities of antennas. In other words, as transmitter and user antenna count grow, the spectral efficiency in a distributed scheme increases at a steeper rate.

In Fig. 4, the ratio of spectral efficiency in the distributed scenario compared to the collocated scheme, Distributed SE / Collocated SE, rises with the increasing number of SBSs. This comparison is tested at different SNRs, specifically at SNR=10 dB, SNR=0dB, and SNR=-5 dB. In all scenarios, the ratio increases as the quantities of SBSs increase. Additionally, the ratio increases with higher SNR values for a specific number of SBSs. This demonstrates that the distributed scheme outperforms the collocated structure concerning spectral efficiency performance.

In Fig. 5, the spectral efficiency is illustrated for various SNR values, with different N_{sym} values being considered.

The results demonstrate that the spectral efficiency increases as the SNR rises in every cases, indicating that the proposed scheme closely approaches the performance of a fully digital structure. This supports the assertion that the proposed hybrid precoding method demonstrates superior performance while maintaining reduced complexity in comparison to a fully digital system. Furthermore, by increasing the N_{sym} values, the system's performance is enhanced. We consider the 2,4, and 8 for N_{sym} in this scenario. We see that the $N_{sym} = 8$ has better performance than others. Note that in this figure, we assume $N_{RF} = 2 * N_{sym}$, which in [13] shows the hybrid precoding scheme can have close performance to fully digital.

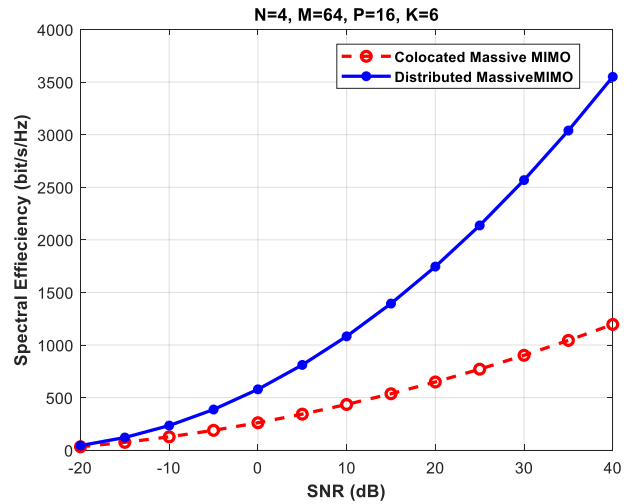


Fig. 3. Comparing the Spectral efficiency of Collocated and Distributed massive multi-user MIMO.

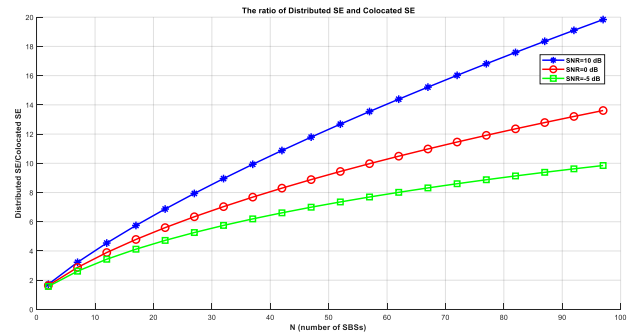


Fig. 4. The ratio of spectral efficiency in distributed massive multi-user case vs collocated scheme.

Fig. 6 analyzes how the quantity of N_{RF} influences the proposed system. The findings indicate that in our proposed structure, the spectral efficiency is close for both $N_{RF} = 2 * N_{sym}$ and $N_{RF} = N_{sym}$, with both approaching the performance of the fully digital case. This shows that our proposed hybrid precoding design can achieve optimal results with reduced complexity. These results hold for various N_{sym} values, consistently yielding favorable outcomes.

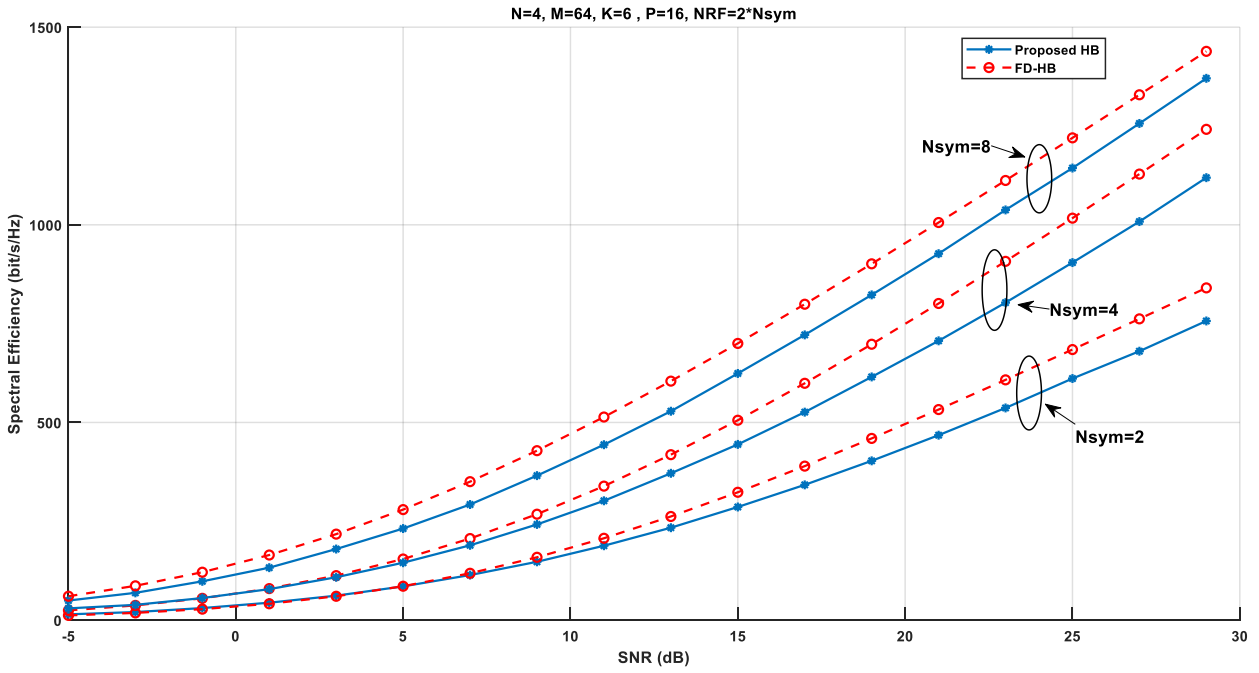


Fig. 5. The spectral efficiency of the proposed hybrid precoding scheme in different SNRs with $N_{RF} = 2 * N_{sym}$.

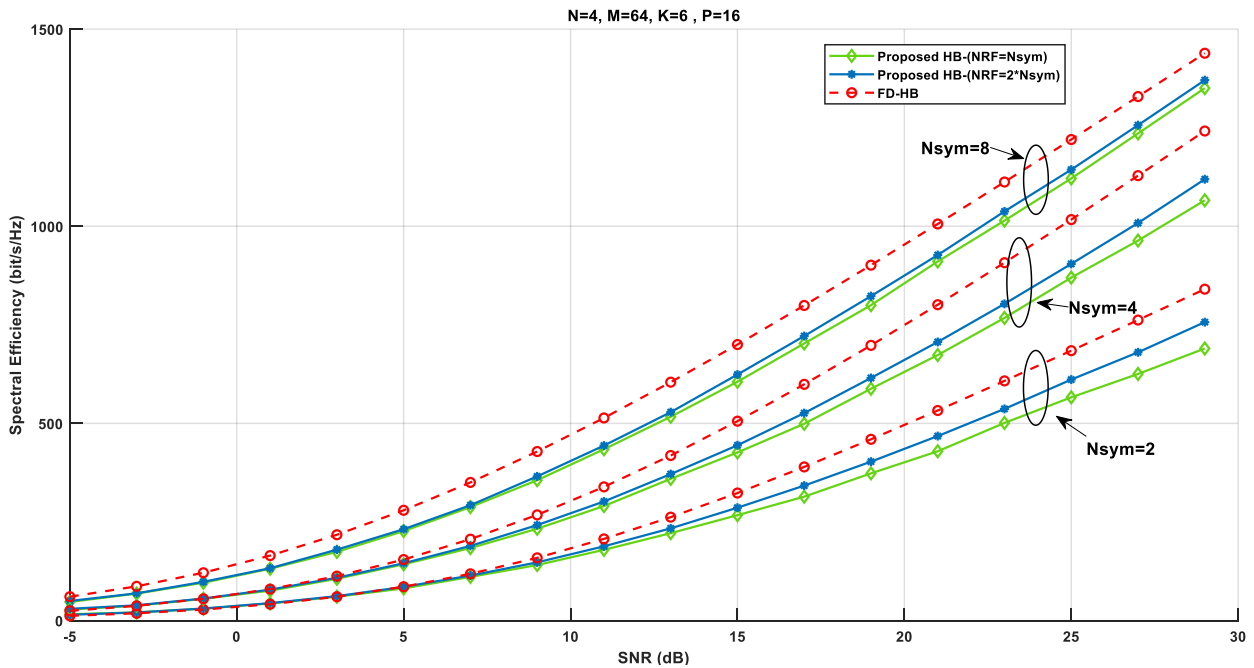


Fig. 6. The comparison of spectral efficiency in the proposed hybrid precoding scheme in two cases: $N_{RF} = 2 * N_{sym}$ and $N_{RF} = N_{sym}$.

8. Conclusion

We conducted a study to evaluate the effectiveness of a two-stage iterative fully connected hybrid precoding technique in distributed massive MU MIMO systems with a focus on enhancing the spectral efficiency in modern wireless communication networks. The incorporation of hybrid precoding methods, which leverage analog and digital processing, offers a potential remedy to address the challenges posed by high-dimensional data and limited hardware resources. Our study focuses on a distributed massive multi-user MIMO system model with the BS divided into multiple SBSs to enhance spatial diversity and signal quality, especially in urban environments with

potential multipath propagation issues. Each SBS is capable of serving users within its proximity to minimize interference and improve throughput. We specifically apply this system model in the mmWave channel and demonstrate that with a substantial increase in the number of antennas in SBS, interference among users can be eradicated. Our primary objective is to maximize spectral efficiency in this system model, leading us to formulate an optimization problem with the total spectral efficiency as the objective function and two constraints on the analog RF precoding matrix and the total transmit power budget. Due to the nonconvex nature of this problem, we propose a two-stage iterative algorithm to solve it. In the first stage, we obtain the optimal digital precoder matrix by assuming the known

analog RF matrix, followed by achieving the optimal analog RF precoding using the optimal digital precoding matrix in the next step. Our iterative algorithm design leverages Lagrange multipliers and KKT conditions in each stage to solve the problem and obtain the desired matrix. Additionally, we assess the complexity of this proposed algorithm and find that it has less complexity compared to other hybrid precoding algorithms that already exist. The simulation results validate our theoretical findings,

demonstrating significant enhancements in spectral efficiency.

This is an Open Access article distributed under the terms of the Creative Commons Attribution License.



References

- [1] T. L. Marzetta, "Noncooperative Cellular Wireless With Unlimited Numbers of Base Station Antennas," *IEEE Trans. Wireless Commun.*, vol. 9, no. 11, pp. 3590-3600, Nov. 2010. doi: 10.1109/TWC.2010.092810.091092.
- [2] E. Björnson, L. Sanguinetti, and M. Kountouris, "Deploying Dense Networks for Maximal Energy Efficiency: Small Cells Meet Massive MIMO," *IEEE J. Select. Areas Commun.*, vol. 34, no. 4, pp. 832-847, Apr. 2016. doi: 10.1109/JSAC.2016.2544642.
- [3] Z. Wei, D. W. K. Ng, J. Yuan, and H.-M. Wang, "Optimal Resource Allocation for Power-Efficient MC-NOMA with Imperfect Channel State Information," *IEEE Trans. Commun.*, vol. 65, no. 9, pp. 3944-3961, Sep. 2017. doi: 10.1109/TCOMM.2017.2717819.
- [4] T. S. Rappaport et al., "Millimeter Wave Mobile Communications for 5G Cellular: It Will Work!" *IEEE Access*, vol. 1, pp. 335-349, May 2013. doi: 10.1109/ACCESS.2013.2260813.
- [5] A. Alkhateeb, G. Leus, and R. W. Heath, "Limited Feedback Hybrid Precoding for Multi-User Millimeter Wave Systems," *IEEE Trans. Wirel. Commun.*, vol. 14, no. 11, pp. 6481-6494, Jul. 2015. doi: 10.1109/TWC.2015.2456944.
- [6] S. Thurpati and P. Muthuchidambaranathan, "Design of Hybrid Precoding for Millimeter-Wave Massive MIMO System," *Wireless Pers. Commun.*, vol. 127, no. 4, pp. 3363-3377, Dec. 2022. doi: 10.1007/s11277-022-09922-5.
- [7] X. Chen et al., "Distributed Stochastic Optimization of Network Function Virtualization," in *GLOBECOM 2017 - 2017 IEEE Global Commun. Conf.*, Singapore: IEEE, Dec. 2017, pp. 1-6. doi: 10.1109/GLOCOM.2017.8254728.
- [8] H. Q. Ngo, E. G. Larsson, and T. L. Marzetta, "Energy and Spectral Efficiency of Very Large Multiuser MIMO Systems," *IEEE Trans. Commun.*, vol. 61, no. 4, pp. 1436-1449, Apr. 2013. DOI: 10.1109/TCOMM.2013.020413.110848.
- [9] N. Li, Z. Wei, H. Yang, X. Zhang, and D. Yang, "Hybrid Precoding for MmWave Massive MIMO Systems with Partially Connected Structure," *IEEE Access*, vol. 5, pp. 15142-15151, Jun. 2017. doi: 10.1109/ACCESS.2017.2720760.
- [10] H. Huang, Y. Song, J. Yang, G. Gui, and F. Adachi, "Deep-Learning-Based Millimeter-Wave Massive MIMO for Hybrid Precoding," *IEEE Trans. Vehic. Techn.*, vol. 68, no. 3, pp. 3027-3032, Jan. 2019. doi: 10.1109/TVT.2019.2893891.
- [11] X. Yu, J.-C. Shen, J. Zhang, and K. B. Letaief, "Alternating Minimization Algorithms for Hybrid Precoding in Millimeter Wave MIMO Systems," *IEEE J. Select. Topics Sign. Proces.*, vol. 10, no. 3, pp. 485-500, Feb. 2016. doi: 10.1109/JSTSP.2016.2523900.
- [12] L. Liang, W. Xu, and X. Dong, "Low-Complexity Hybrid Precoding in Massive Multiuser MIMO Systems," *IEEE Wirel. Commun. Lett.*, vol. 3, no. 6, pp. 653-656, Jun. 2014. doi: 10.1109/LWC.2014.2357053.
- [13] F. Sohrabi and W. Yu, "Hybrid Digital and Analog Beamforming Design for Large-Scale Antenna Arrays," *IEEE J. Select. Topics Sign. Proces.*, vol. 10, no. 3, pp. 501-513, Feb. 2016. doi: 10.1109/JSTSP.2016.2524419.
- [14] X. Zhao, T. Lin, Y. Zhu, and J. Zhang, "Partially-Connected Hybrid Beamforming for Spectral Efficiency Maximization Via a Weighted MMSE Equivalence," *IEEE Trans. Wirel. Commun.*, vol. 20, no. 12, pp. 8218-8232, Dec. 2021. doi: 10.1109/TWC.2021.3098712.
- [15] M. Kanaka Chary, C. H. Vamshi Krishna, and D. Rama Krishna, "Accurate channel estimation and hybrid beamforming using Artificial Intelligence for massive MIMO 5G systems," *AEU - Int. J. Electr. Commun.*, vol. 173, Jan. 2024, Art. no. 154971, doi: 10.1016/j.aeue.2023.154971.
- [16] S. Thurpati, M. Mudavath, and P. Muthuchidambaranathan, "Performance Analysis of Linear Precoding in Downlink Based on Polynomial Expansion on Massive MIMO Systems," *J. Phys.: Conf. Ser.*, vol. 2062, no. 1, Nov. 2021, Art. no. 012006, doi: 10.1088/1742-6596/2062/1/012006.
- [17] S. Thurpati, M. Mudavath, and P. Muthuchidambaranathan, "Design of Hybrid Beamforming for Multiuser MIMO mmWave Systems Using Deep Learning," *Wirel. Pers. Commun.*, vol. 135, no. 3, pp. 1747-1760, Apr. 2024, doi: 10.1007/s11277-024-11159-3.